Atmospheric Environment 45 (2011) 1483–1490

Contents lists available at ScienceDirect

Atmospheric Environment

journal homepage: www.elsevier.com/locate/atmosenv

Sensitivity of contrail coverage and contrail radiative forcing to selected key parameters

C. Frömming [a,*], M. Ponater [a], U. Burkhardt [a], A. Stenke [b], S. Pechtl [c], R. Sausen [a]

[a] Deutsches Zentrum für Luft- und Raumfahrt, Institut für Physik der Atmosphäre, Oberpfaffenhofen, Germany
[b] Institute for Atmospheric and Climate Science, Eidgenössische Technische Hochschule (ETH), Zürich, Switzerland
[c] Deutsches Patent- und Markenamt, München, Germany

ARTICLE INFO

Article history:
Received 16 June 2010
Received in revised form
3 November 2010
Accepted 24 November 2010

Keywords:
Air traffic
Aviation
Climate impact
Contrail coverage
Radiative forcing
Optical depth

ABSTRACT

Estimates of global mean radiative forcing of line-shaped contrails are associated with a high level of uncertainty. Recent estimates for present day air traffic range from 5.4 mWm^{-2} to 25.6 mWm^{-2}. The aim of this research paper is to systematically study the sensitivity of contrail radiative forcing to selected key parameters and to highlight the most important factors for this large uncertainty range, while employing an improved version of the ECHAM climate model.

The dominating parameters on contrail radiative forcing are found to be the detection threshold used for calibrating contrail coverage to observations, and the mean optical depth. Assuming a detection threshold of 0.05 instead of 0.02 yields an increase of the total coverage, resulting in a 146% increase of global mean contrail radiative forcing. Employing a globally constant optical depth of up to 0.3, increases the net radiative forcing by 140% over the reference case which has a mean optical depth of 0.08. An upgraded parameterisation of potential contrail coverage yields a significantly larger amount of tropical contrails, increasing the contrail radiative forcing by 53%. The calibration to an alternative observation region along with the assumption of a higher visibility threshold yields an increase of the radiative forcing by 46%. Moderate sensitivity of global contrail radiative forcing (~15%) is found for an improvement of model climate and for changes in particle shape. The air traffic inventory, air traffic density parameter, and the diurnal variation of air traffic have only a small effect on global and annual mean contrail radiative forcing, but their influence on regional and seasonal contrail radiative forcing may nevertheless be important.

1. Introduction

Contrails are line-shaped ice clouds which form as a consequence of water vapour emissions and heat released from aircraft if ambient conditions at flight levels are suitable. Linear contrails can persist for many hours and may evolve into contrail cirrus clouds. Within this study, only linear contrails will be considered. These additional clouds influence the Earth's radiation budget and thereby contribute to climate change. Air traffic in total contributes only 3.5–4.9% to the total anthropogenic radiative forcing (Lee et al., 2009), whereof up to one-fifth originates from linear contrails. Nevertheless, the climate impact of air traffic is of major concern, as this sector is one of the fastest growing anthropogenic emission sectors with growth rates of about 5% per year (Airbus, 2009).

Although contrails have received special attention in aviation climate research, large uncertainties associated with the radiative impact of linear contrails and aged contrail cirrus remain. The IPCC (Penner et al., 1999) gave an uncertainty range for the radiative forcing of linear contrails of 5 mWm^{-2} to 60 mWm^{-2} for the air traffic of 1992. More recent studies determined the radiative forcing of linear contrails ranging from 2.8 mWm^{-2} (Stuber and Forster, 2007) to 12 mWm^{-2} (Rap et al., 2010) for air traffic in 2002 and from 5.4 mWm^{-2} to 25.6 mWm^{-2} for air traffic in 2005 (Lee et al., 2009). This wide range of global mean contrail radiative forcing values is associated with deviating assumptions of important key factors and different methodologies.

The aim of this study is to systematically examine the influence of various key factors on contrail coverage and radiative forcing within a global climate model. Aspects like the model climate, the parameterisation of potential contrail coverage, the contrail optical depth, the detection threshold of contrail observations, the calibration region, the air traffic inventory, the air traffic density

* Corresponding author. Tel.: +49 8153 283022; fax: +49 8153 281841.
E-mail address: christine.froemming@dlr.de (C. Frömming).

1352-2310/$ – see front matter © 2010 Elsevier Ltd. All rights reserved.
doi:10.1016/j.atmosenv.2010.11.033

parameter, the particle shape, and the diurnal variation of air traffic are investigated. The relative importance of these parameters is studied and discussed in the context of the large uncertainty range of previous contrail studies.

2. Methodology

2.1. Model description and evaluation

The parameterisation for line-shaped contrails developed by Ponater et al. (2002) has been applied in the ECHAM4.L39(DLR) climate model (E39SLT) and in an upgraded version ECHAM4.L39 (DLR)/ATTILA (E39A) (Reithmeier and Sausen, 2002; Stenke et al., 2008). The Lagrangian transport scheme in E39A can maintain steeper and more realistic gradients of highly variable tracers than the semi-Lagrangian transport scheme in E39SLT. E39A shows a significant reduction of systematic errors of temperature and humidity in the upper troposphere and lower stratosphere (UTLS) (Stenke et al., 2008). In a detailed comparison Obermaier (2007) concluded that water vapour observations are reproduced better with E39A than with E39SLT. Fig. 1 shows vertical profiles of the simulated annual mean relative humidity with respect to ice for northern mid and polar latitudes in comparison with ERA40 data. The reduction of the humidity bias entails a reduction of the temperature bias in the UTLS through radiative effects. The representation of both, temperature and humidity, is crucial for the atmospheric susceptibility to contrails according to the thermodynamic theory of contrail formation (e.g., Schumann, 1996), hence, more realistic results of contrail coverage and their properties are expected.

The potential contrail coverage, defined as the atmospheric ability to form contrails (Sausen et al., 1998), is calculated instantaneously within the climate model at each time step. The three-dimensional actual contrail coverage is calculated from the product of potential contrail coverage and air traffic density. The visible contrail coverage (optical depth $\tau > 0.02$) is randomly overlapped over all model levels and is then adjusted to regionally observed contrail coverage (Bakan et al., 1994) by means of a calibration factor. Taking into account the increase of air traffic in this region since the original observation dates, the visible contrail coverage over Europe and the North-East Atlantic region is calibrated to a value of 0.75%, similarly to Rädel and Shine (2008). Within the present study, 3-year simulations of year 2000 conditions are analysed.

The radiative effect of contrails is determined by the fractional coverage, the optical properties of contrails, the contrail temperature, and the change of the system albedo. As in previous studies, the stratosphere-adjusted radiative forcing has been calculated online using the method developed by Stuber et al. (2001). Because longwave scattering is not included in the ECHAM4 standard radiation scheme, the longwave radiative forcing of optically very thin contrails is systematically underestimated by 25%, therefore it has been corrected as suggested in Marquart and Mayer (2002), unless stated otherwise.

Recently, a benchmark test involving five different radiative transfer models was performed by Myhre et al. (2009). A homogeneously distributed "contrail coverage" of 1% with $\tau = 0.3$ was assumed globally at an altitude of 11 km in all participating models. A substantial model dependency was found in the distribution and magnitude of contrail net radiative forcing, not only because of different radiation codes, but also due to the differing background climate. The most distinct differences were found in regions where natural cloud cover is large. Global mean net radiative forcing varied by ±25% around the multi-model mean of 144 mWm^{-2} with even larger deviations in the long- and shortwave forcing components. In order to evaluate the performance of the ECHAM4 radiation scheme for contrail studies, this benchmark test has been reproduced with E39A. Fig. 2 shows the respective distribution of the annual mean contrail net radiative forcing. The largest radiative impact occurs over regions with few natural clouds, e.g. deserts and subtropical oceans, while low net contrail forcing is found along with high natural cloud cover and low surface temperatures. The results are qualitatively consistent with the distributions presented in Myhre et al. (2009). The global mean net radiative forcing for 1% homogeneous contrail coverage is 140 mWm^{-2} (210 mWm^{-2} and −70 mWm^{-2} for the uncorrected longwave and shortwave components, respectively) and thus very close to the multi-model mean given by Myhre et al. (2009). If the longwave radiative forcing contribution was corrected for the systematic underestimation, the

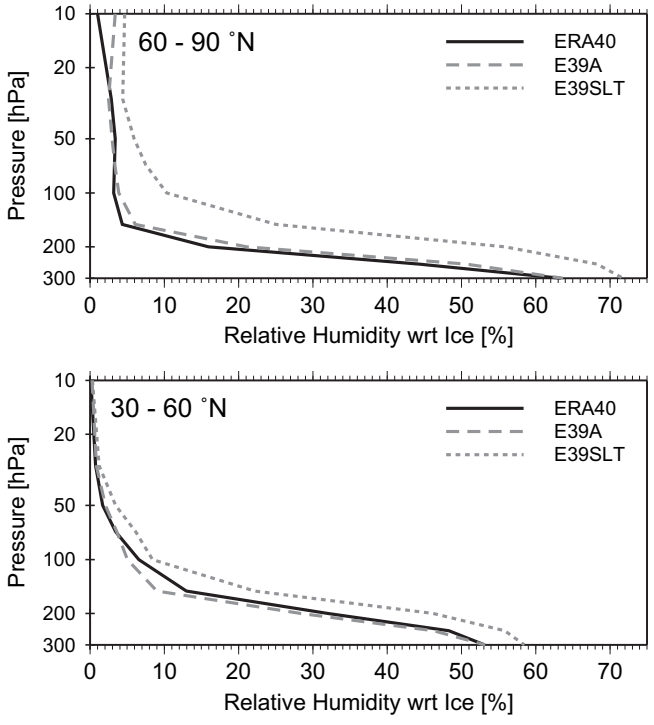

Fig. 1. Relative humidity with respect to ice for northern hemisphere polar (top) and mid latitudes (bottom) for E39A and E39SLT in comparison with ERA40 data.

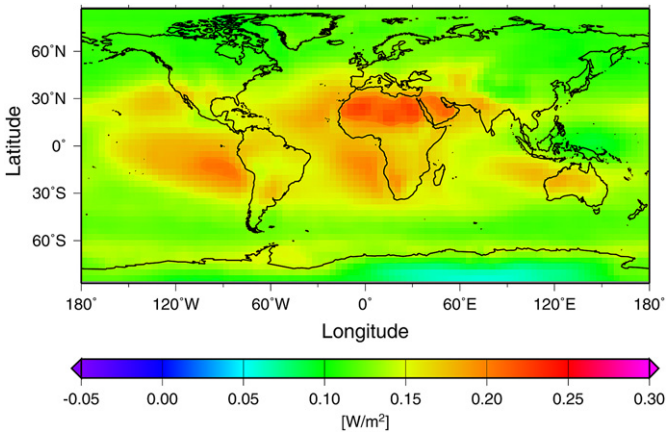

Fig. 2. Annual mean net radiative forcing [Wm^{-2}] for 1% homogeneously distributed "contrail coverage" representing a benchmark test for the ECHAM radiation scheme (Please note the slightly different colour scale compared with Myhre et al., 2009.).

net forcing would increase to 210 mWm^{-2}, reaching the upper end of the range of results from Myhre et al. (2009). This may be an indication that the correction of the longwave contrail forcing is required for very small optical depths around 0.1 but not necessarily for optical depths of 0.3 as assumed in the benchmark test, however, subsequent studies are needed to confirm this.

2.2. Air traffic data

Two inventories of air traffic density are employed within this study, the TRADEOFF 2000 and the AERO2K (Eyers et al., 2004) inventory. Both have been used previously in aviation climate impact studies (e.g., Gauss et al., 2006; Rädel and Shine, 2008) and are used here to investigate the sensitivity of contrail coverage with respect to the chosen air traffic inventory.

The TRADEOFF inventory was generated on the basis of flight track data of 1991/1992. The global fleet is represented by 16 aircraft-engine combinations. Fuel flow profiles for these aircraft types were computed by means of the commercial aircraft performance model PIANO.[1] A payload of 70% was assumed and cruise altitudes were prescribed by mission distance and aircraft type, as specified from an analysis of real flight data. Assigning a global database of aircraft movements to corresponding precalculated fuel-flow profiles under the assumption of great circle routes between city pairs, resulted in three-dimensional inventories with a horizontal resolution of $1^\circ \times 1^\circ$ and a vertical resolution of 2000 ft (610 m). The TRADEOFF inventory for the year 2000 has been obtained by scaling the basic inventory from 1992 to the year 2000, assuming the IS92f scenario (Leggett et al., 1992) and a 1.1% fuel efficiency improvement per year.

As an alternative, the AERO2K inventory is used, which is based on radar data from the year 2002 for North America, Europe, and the North Atlantic reporting actual longitude, latitude and altitude during the flight. These data comprise about 70% of the inventory. Air traffic data for the rest of the world include scheduled flights only, which were supplemented by routing and performance information if available. Fuel flow data were calculated by means of PIANO using 40 representative aircraft types. The take-off weight was estimated according to the particular mission range plus reserve fuel and a payload of 60.9% was assumed. Information about waypoints and flight altitudes were taken into account if available from radar data and step-climbs were implemented if appropriate. If no information about waypoints and flight altitudes was available, the flight track including its altitude profile was based on assumptions taking restricted airspace into consideration. This implies a different degree of data quality for different regions of the world, however it is a substantial improvement compared to the assumption of great circle routes in the TRADEOFF inventory.

Both inventories do not include the diurnal cycle of air traffic. The global mean flight distances show a difference of more than 20%, which is caused by the different base years and differences in the underlying data and methodology. The TRADEOFF 2000 inventory comprises 25.1×10^9 km/a and the AERO2K inventory 32.9×10^9 km/a. The annual and global mean vertical distribution of flown distances is displayed in Fig. 3, revealing some characteristic differences between the two inventories. These differences are caused by different assumptions about flight altitudes and additional aircraft types (particularly additional smaller planes flying at lower altitudes in the AERO2K inventory). The geographical distribution of air traffic density shows differences, too, which are mainly caused by the usage of great circle routes versus waypoint data.

[1] http://www.piano.aero.

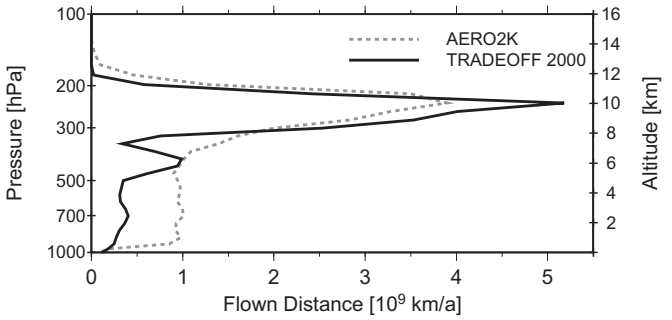

Fig. 3. Altitudinal distribution of air traffic in the AERO2K and TRADEOFF 2000 inventory.

3. Results

3.1. Contrail coverage, properties and radiative forcing

Table 1 gives an overview over the reference simulation (REF) and all sensitivity experiments which are explained in the following sections. In REF the total global contrail coverage amounts to 0.19%, and the total visible contrail coverage to 0.09%. The geographical distribution of total contrail coverage is shown in Fig. 4. The annual global mean optical depth of visible contrails is 0.08 and of all contrails 0.05, respectively. The global annual mean contrail radiative forcing amounts to 5.9 mWm^{-2}, with longwave and shortwave components of 7.9 mWm^{-2} and -2.0 mWm^{-2}, respectively. The geographical distribution of the radiative forcing is shown in Fig. 5 with maximum net radiative forcing values of more than 100 mWm^{-2} found over Europe and the USA. Table 2 summarizes annual global mean results of contrail coverage, optical depth and radiative forcing for all simulations.

Table 1
Overview of simulations and sensitivity experiments.

Experiment	Short description
REF	Reference simulation using E39A, TRADEOFF 2000, flown distance, no diurnal cycle, potential contrail coverage according to Ponater et al. (2002), variable optical depths, calibration region according to Bakan et al. (1994), visibility threshold $\tau = 0.02$, hexagonal particles.
SLT	Sensitivity experiment, as REF but using E39SLT instead of E39A.
AERO2K	Sensitivity experiment, as REF but using the AERO2K inventory instead of TRADEOFF 2000.
POTCOV	Sensitivity experiment, as REF but using the potential contrail coverage according to Burkhardt et al. (2008).
BAK 0.05	Sensitivity experiment, as REF but using a visibility threshold of $\tau = 0.05$ for calibration.
USA 0.05	Sensitivity experiment, as REF but using a visibility threshold of $\tau = 0.05$ and the calibration region according to Palikonda et al. (2005).
TAU 0.08	Sensitivity experiment, as AERO2K but with a constant optical depth of $\tau = 0.08$.
TAU 0.12	Sensitivity experiment, as AERO2K but with a constant optical depth of $\tau = 0.12$.
TAU 0.15	Sensitivity experiment, as AERO2K but with a constant optical depth of $\tau = 0.15$.
TAU 0.3	Sensitivity experiment, as AERO2K but with a constant optical depth of $\tau = 0.3$.
FUEL	Sensitivity experiment, as SLT but using fuel consumption as air traffic density parameter instead of flown distance.
SHAPE	Sensitivity experiment, as SLT but using spherical particles instead of hexagonal particles.
DIURNAL	Sensitivity experiment, as SLT but including the diurnal cycle of air traffic.

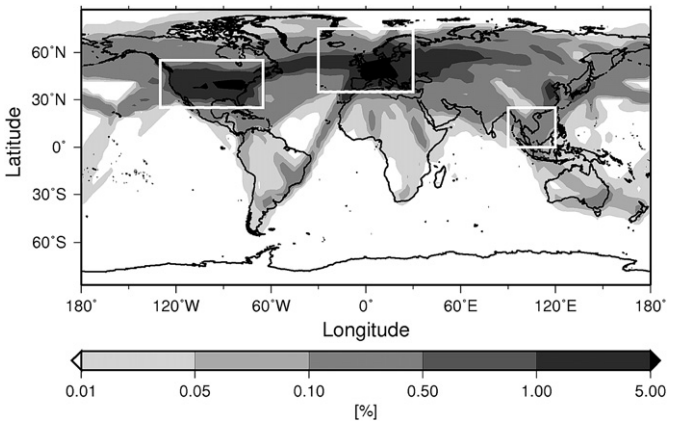

Fig. 4. Annually averaged total contrail coverage [%] in the reference simulation using the TRADEOFF 2000 inventory. The boxes indicate regions which are used for calibration or for comparison with observations.

3.2. Sensitivity to model climatology

Marquart et al. (2003) found an underestimation of global contrail coverage of up to 20% resulting from systematic temperature and humidity biases in E39SLT. As these biases are reduced in E39A an improvement of contrail coverage and contrail parameters is anticipated. Fig. 6 shows the annually averaged zonal mean potential contrail coverage in REF and the difference of potential contrail coverage between REF and SLT. The potential contrail coverage is reduced in REF in the UTLS with maximum reduction just above the tropopause.

The changes of the vertical profile of potential contrail coverage in combination with the calibration procedure yield a systematic relocation of contrails to lower levels in REF compared with SLT, with warmer and moister formation conditions, which should result in contrails with higher ice water content and higher optical depth. However, as less condensable water is available in REF in the UTLS contrails have lower mean optical depth compared with SLT. Fig. 7 shows probability density functions (PDFs) and cumulative distribution functions of contrail optical depths for SLT and REF. SLT shows more contrails with higher optical depths and a slightly wider PDF than REF. This results in global mean optical depths of 0.08 of all contrails, and of 0.12 of visible contrails in SLT (Table 2). The visible contrail coverage over Europe and the Northern Atlantic is adjusted to the same value in both model versions, however, the global coverage of subvisible contrails (total coverage minus visible coverage) is about twice as high in REF compared with SLT (Table 2). Although optically thin contrails have a comparatively small impact on radiation e.g., (Meerkötter et al., 1999), the increase in subvisible contrail coverage by a factor of two results in an increase in contrail radiative forcing from 5.2 mWm^{-2} in SLT to 5.9 mWm^{-2} in REF (+14%), mainly through an increase in longwave radiative forcing (Table 2).

Another potential reason for the increase in longwave radiative forcing between the two model versions is the general decrease in relative humidity in the upper troposphere in REF (Fig. 1). Reduced water vapour results in an increased upward thermal flux which may increase the longwave radiative forcing by contrails as discussed in Meerkötter et al. (1999). A further reason could be changes in natural cloud coverage which influences the overlap between natural clouds and contrails compared with SLT.

3.3. Sensitivity to air traffic inventory

The influence of differences in the vertical and horizontal distribution of air traffic on contrail coverage is investigated by employing two different air traffic inventories in otherwise identical simulations: the TRADEOFF inventory and the AERO2K inventory. The visible contrail coverage over Europe and the Northern Atlantic region has been calibrated to 0.75% in both simulations. The total global contrail coverage deviates by 5% and the global mean radiative forcing deviates by 3% between REF and AERO2K (Table 2). Regional and seasonal coverages, however, show considerable differences. Fig. 8 shows monthly mean coverages of visible contrails over the USA in comparison with observations (Palikonda et al., 2005) derived from satellite data using automatic contrail detection (Mannstein et al., 1999). These observations indicate an annual mean coverage over the USA of 0.87% for the year 2001, substantially smaller than previous results (Minnis et al., 2000) for the year 1993 for the same region. As nighttime coverage was not included in the satellite observations, Palikonda et al. (2005) suggest to correct their daytime values, yielding an annual mean corrected coverage of 0.62%. An additional correction factor associated with false detection rates has been identified in Palikonda et al. (2005), but has not been included within the present study as its size and representativeness is uncertain. The observed seasonal cycle with minimum contrail coverage in summer and a broad maximum between November and May is reproduced very well in REF, and the seasonal amplitude has improved significantly compared with SLT (Fig. 8). In all months

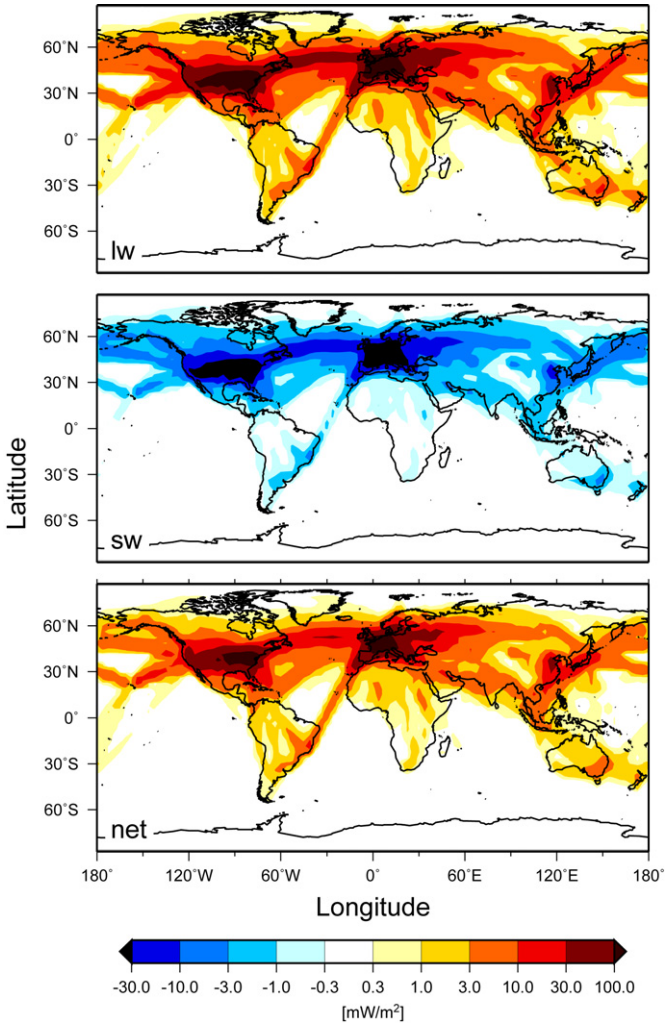

Fig. 5. Annual mean longwave, shortwave and net radiative forcing [mWm^{-2}] of contrails at the tropopause in the reference simulation.

Table 2
Global annual mean values of visible and total contrail coverage [%], optical depths of visible contrails, contrail shortwave (sw), longwave (lw) and net radiative forcing (RF) [mWm^{-2}] for the reference case and various sensitivity experiments.

	Visible coverage	Total coverage	Optical depth	sw RF	lw RF	net RF	net RF change
REF	0.09	0.19	0.08	−2.0	7.9	5.9	
SLT	0.08	0.13	0.12	−2.1	7.3	5.2	−12%[a]
AERO2K	0.09	0.18	0.08	−2.0	7.7	5.7	−3%[a]
POTCOV	0.10	0.22	0.09	−3.0	12.0	9.0	+53%[a]
BAK 0.05	0.09	0.45	0.13 (>0.05)	−5.0	19.5	14.5	+146%[a]
USA 0.05	0.06	0.27	0.13 (>0.05)	−3.0	11.6	8.6	+46%[a]
TAU 0.08	0.09	0.18	0.08	−2.5	9.3	6.8	+19%[b]
TAU 0.12	0.09	0.18	0.12	−3.6	13.2 (9.9[c])	9.6 (6.3[c])	+10%[b, c]
TAU 0.15	0.09	0.18	0.15	−4.5	16.1 (12.1[c])	11.6 (7.6[c])	+33%[b, c]
TAU 0.3	0.09	0.18	0.3	−8.4	29.5 (22.1[c])	21.1 (13.7[c])	+140%[b, c]
FUEL	0.09	0.14		−2.4	8.4	6.3	+7%[d]
SHAPE	0.08	0.13		−1.4	7.3	5.9	+14%[d]
DIURNAL	0.08	0.13		−2.4	7.3	4.9	−6%[d]

[a] With respect to REF.
[b] With respect to AERO2K.
[c] Without correction of lw radiative forcing.
[d] With respect to SLT.

except June and July, the model results are somewhat higher than the corrected observations.

The annual cycle of contrails over the USA using the AERO2K inventory deviates from REF and from observations particularly in summer (Fig. 8). In the AERO2K inventory air traffic occurs at somewhat higher atmospheric levels which reside in the lowermost stratosphere in winter, but in the upper troposphere in summer, allowing more frequent contrail formation then. This yields a less pronounced minimum in summer than with the TRADEOFF inventory, highlighting the significance of the exact representation of flight altitudes in air traffic inventories and the correct representation of the tropopause height in contrail modelling studies, particularly for regional and seasonal comparisons. Over the Thailand region, contrail coverage is strongly underestimated with both inventories as well as in SLT (Fig. 9).

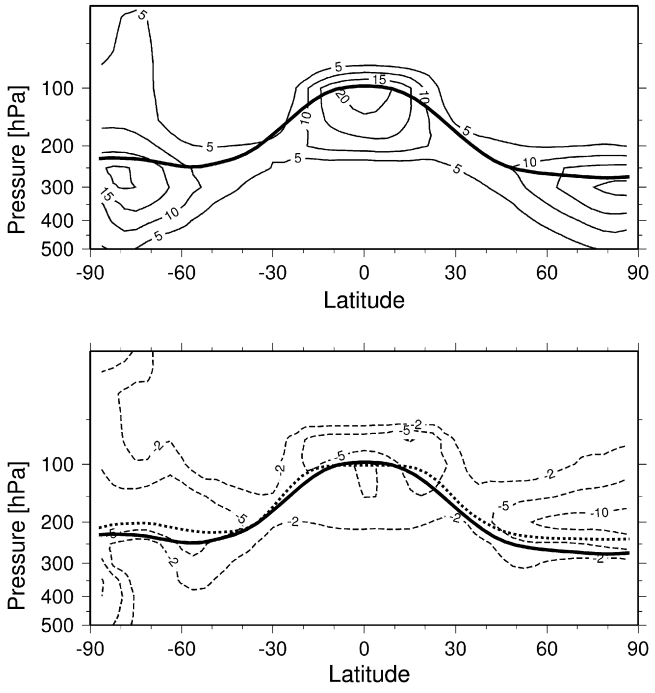

Fig. 6. Zonal annual mean potential contrail coverage [%] in REF (top) and difference of potential contrail coverage [%] in REF minus SLT (bottom), solid isolines indicate positive, dashed isolines indicate negative values. The bold lines indicate the annual mean tropopause height in REF (solid) and SLT (dotted).

3.4. Sensitivity to potential contrail parameterisation

In order to demonstrate the importance of the exact formulation of the parameterisation, an upgraded parameterisation of potential contrail coverage (Burkhardt et al., 2008) has been employed alternatively (POTCOV) to the original formulation. The new formulation is derived using the same PDF of the total water mixing ratio as inherent in the natural cloud scheme and is therefore more consistent with the latter. For natural cirrus formation, the homogeneous freezing threshold is assumed instead of water saturation as in the original parameterisation, which overcomes an underestimation of the grid mean critical relative humidity for contrail formation. In total this results in higher potential contrail coverage in regions with high relative humidity and a decrease in regions with low relative humidity. This yields an increase of total global contrail coverage by 16% (Table 2), which is mainly caused by additional tropical contrail coverage enhanced by a factor of about 2. In comparison with observations in the tropics, e.g. over Thailand (Meyer et al., 2007), the new parameterisation induces considerable improvements over the original parameterisation, which simulates significantly lower contrail coverage than observed

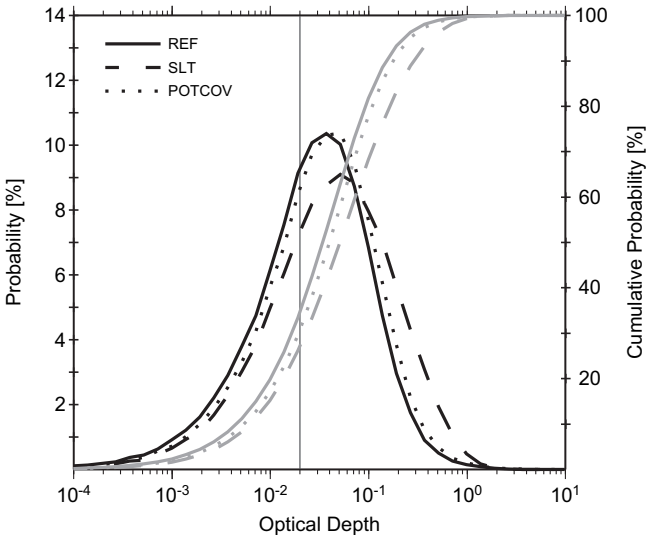

Fig. 7. Probability density function (black) and distribution function (grey) of global contrail optical depths in REF (solid), SLT (dashed) and POTCOV (dotted). The vertical dark grey line indicates the visibility threshold of 0.02.

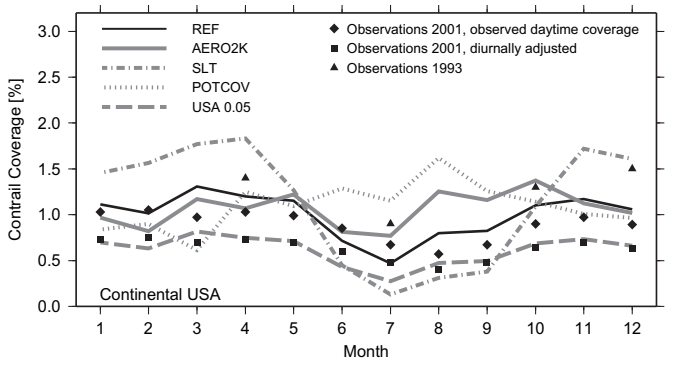

Fig. 8. Annual cycle of visible contrail coverage [%] over the United States for certain model configurations in comparison with observations.

(Fig. 9). This improvement has already been shown by Burkhardt and Kärcher (2009) for young contrail cirrus, and is confirmed by the parameterisation for linear contrails used here.

However, the revised parameterisation does not automatically lead to better agreement between model and observations everywhere (Fig. 8). The differences in the seasonal cycle of contrail coverage over the USA can be attributed to differences in the seasonal characteristics of the potential contrail coverage in REF and POTCOV. The new parameterisation favours contrail formation immediately below the tropopause, which in summer coincides frequently with main flight altitudes, while during winter the tropopause is located at lower levels, below the main flight altitudes, prohibiting contrail formation in many cases. Thus, the contrail coverage is larger in summer in POTCOV. However, seasonal cycles of contrail coverage were in accordance with observations when this parameterisation was employed within E39SLT using the AERO2K inventory (Burkhardt and Kärcher, 2009). Differences between their simulation and POTCOV arise from the combination of differences in the tropopause height, air traffic inventory and contrail parameterisation, indicating that the validation of seasonal contrail coverage is not conclusive.

As more contrails form at higher humidity conditions, the global mean visible optical depth increases by about 10% compared with REF (Table 2 and Fig. 7). Both factors, the increase of contrail coverage and mean optical depths yield an increase of global mean net radiative forcing by 53% (Table 2).

3.5. Sensitivity to optical depth, calibration region and visibility threshold

Several previous publications (e.g., Minnis et al., 1999; Forster et al., 2007) have stated that the large uncertainty range of global

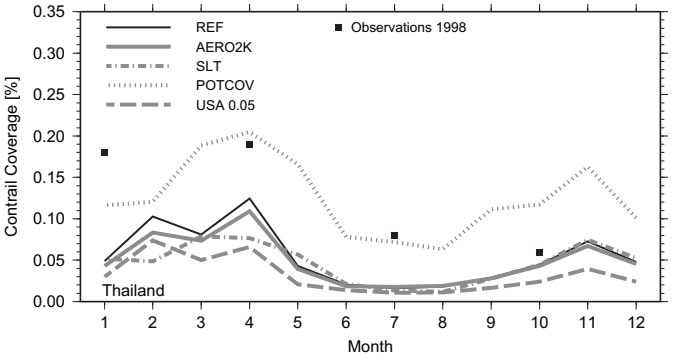

Fig. 9. Annual cycle of visible contrail coverage [%] over Thailand for certain model configurations in comparison with observations.

contrail radiative forcing estimates can mainly be attributed to insufficient knowledge of contrail optical depths. Studies employing a globally uniform optical depth found an almost linear relationship between radiative forcing and optical depth (e.g., Meerkötter et al., 1999; Rädel and Shine 2008). To confirm this relation in E39A, the optical depth of all visible contrails was set to a fixed value of 0.08, 0.12, 0.15, and 0.3, respectively. For these experiments, the AERO2K inventory was used, allowing an optimal comparison with Rädel and Shine (2008). The radiative forcing was calculated for visible contrails only, yielding a net radiative forcing of 6.8 mWm^{-2}, 9.6 mWm^{-2}, 11.6 mWm^{-2} and 21.1 mWm^{-2}. Similar to other studies, only a slight deviation from linearity is found. The results from Rädel and Shine (2008) who found a net radiative forcing of 5.9 mWm^{-2} and 9.8 mWm^{-2} for $\tau = 0.15$ and 0.3 deviate by less than 30% from the present results, if compared with the non-corrected radiative forcing. This is a further indication, that the necessity of the longwave radiative forcing correction (Section 2.1) applies only to very small contrail optical depths, and that the performance of the broadband radiation scheme of ECHAM compares well to more sophisticated line-by-line radiative transfer models for $\tau = 0.15$ and higher. Overall, this confirms the mean optical depth as one of the major factors controlling contrail radiative forcing.

In the standard simulations τ is variable in space and time and the mean optical depth results from the PDF of τ, while the corresponding contrail coverage further depends on the detection threshold assumed for calibration. Kärcher et al. (2009) compared PDFs of τ derived from a microphysical model with the corresponding observations over the USA from Palikonda et al. (2005). They concluded that in this particular case automatic contrail detection misses 89% of contrails with $\tau < 0.05$, 50% of contrails with $0.05 < \tau < 0.1$, and 11% of contrails with $0.1 < \tau < 0.2$. This implies that a detection threshold of 0.02, as assumed for the calibration of contrail coverage to observations, may be too low. In a sensitivity experiment (USA 0.05) we assume a detection threshold of 0.05 and calibrate the simulated coverage over the USA to observations from Palikonda et al. (2005), neglecting that some contrails have also been missed by satellite observations with $0.05 < \tau < 0.1$. The visible global contrail coverage decreases by 33% compared with REF, which can be attributed to the comparatively low coverages determined by Palikonda et al. (2005). The total global contrail coverage increases by 42%, as the contribution of subvisible contrails to the total coverage increases substantially. The global mean optical depth of visible contrails increases to 0.13, and the global mean net radiative forcing increases by 46% compared with the reference simulation.

In a second sensitivity study (BAK 0.05), a detection threshold of $\tau = 0.05$ was assumed but the coverage of visible contrails was calibrated to the usual region over Europe and the North-East Atlantic (Bakan et al., 1994) as in REF. This again yields a strong increase of the fraction of subvisible contrails and an increase of the total global coverage by 137%. The global mean optical depth of visible contrails ($\tau > 0.05$) increases to 0.13, and the global mean contrail radiative forcing increases by 146% (Table 2).

It has been argued that optically very thin contrails, which are frequently missed by automatic contrail detection algorithms (Kärcher et al., 2009), have a negligible climate impact anyway (e.g., Meyer et al., 2007). However, the large amount of optically very thin contrails (Fig. 7) may make up for this. To quantify the contribution of contrails with different optical depths to the total coverage and radiative forcing some extra simulations were performed in which the radiative forcing and coverage is only calculated for contrails within defined optical depth classes (Table 3). Optically thin contrails have a smaller specific radiative impact, however, contrails with $\tau < 0.05$ contribute 79% to the total contrail

coverage and 36% to the total radiative forcing. In contrast, contrails with $\tau > 0.1$ contribute only 6% to the contrail coverage but 37% to the contrail radiative forcing, indicating their significantly larger specific radiative impact. Obviously, none of the optical depth classes and the corresponding radiative effects is negligible, which again highlights the need for observations along with reliable visibility thresholds, preferably for several regions of the world.

3.6. Sensitivity to other parameters

Further parameters which may influence contrail coverage and radiative forcing have been studied using the E39SLT model only. They have partially been published earlier and are only briefly summarized here to put their relative importance in context of other effects discussed within the present study.

Fichter et al. (2005) studied the sensitivity with respect to the air traffic density parameter used. They found an increase of contrail coverage by 11% and of radiative forcing by 7% when using fuel consumption instead of flown distance (Table 2), calibrating to observations of Bakan et al. (1994) in both cases. This increase is caused by the predominantly smaller planes travelling over continental Europe (the larger part of the calibration region) with comparatively smaller fuel consumption per distance flown, yielding an increase of the calibration factor.

Non-spherical particles like hexagonal plates cause significantly larger reflection of shortwave radiation, yielding smaller net radiative forcing than spherical contrail particles. Marquart (2003) studied the influence of contrail particle shape and found a reduction of the shortwave radiative forcing by more than 30% for spherical particles, whereas the influence on longwave radiative forcing was negligible. In total this resulted in an increase of the net radiative forcing by 14% (Table 2). Other studies, using more sophisticated radiative transfer models with higher spectral resolution found a larger sensitivity with respect to particle shape. Meerkötter et al. (1999) reported an increase of net radiative forcing by 30% for mid latitudes summer conditions. Rap et al. (2010) found an increase of the global mean net radiative forcing by almost 70%. In situ observations indicate, that most particles in young contrails are non-spherical, with a predominant shape of hexagonal plates and columns (e.g., Goodman et al., 1998), but also spherical particles have been observed (Schröder et al., 2000).

The diurnal variation of air traffic is very important in regional contrail studies (Stuber et al., 2006), but also in global contrail studies a reduction of contrail radiative forcing by almost 20% was found for an inclusion of the diurnal air traffic variation (e.g., Stuber and Forster, 2007). When taking the daily-cycle of air traffic into account Marquart (2003) found an increase of the global mean shortwave radiative forcing by 14%, but only little influence on the global mean longwave radiative forcing. The net radiative forcing was reduced by 6% compared to the reference case (Table 2), however, regional and seasonal effects are significantly larger. The effect of the daily traffic variation is much more pronounced in winter, reducing the net radiative forcing by 12% in January but by only 4% in July. Furthermore, in regions with significantly higher daytime than nighttime traffic (e.g. Europe, USA) the shortwave radiative forcing component is enhanced, yielding a lower net radiative forcing when including the daily cycle of air traffic. The opposite is true along flight corridors with high nighttime traffic. Because of these seasonal and regional effects it is recommended to include the diurnal variation of air traffic in future studies, particularly when focusing on temporally or spatially resolved data.

Table 3
Contribution of optical depth classes to global contrail coverage and global contrail radiative forcing.

Optical depth classes	Contribution to global contrail coverage [%]	Contribution to global contrail radiative forcing [%]
0–0.02	53	10
0.02–0.05	26	26
0.05–0.1	15	27
>0.1	6	37

4. Discussion and conclusion

The model simulations and sensitivity experiments presented within this study aimed at quantifying the influence of selected key parameters on contrail coverage and contrail optical depth in global climate studies. Their relative importance was assessed in terms of their impact on global contrail radiative forcing.

The largest increase of global contrail radiative forcing over the reference case was found for shifting the detection threshold for calibration from 0.02 to 0.05 (+146%), which strongly enhances the coverage with sub-visible contrails and thereby the total coverage. However, if the same contrail detection threshold is used for calibration to observations over the USA, the radiative forcing increases by only +46%. Both observational data sets are based on different methods and have been developed independently, however, the detection threshold is not exactly known in either case. Because of the large influence of the detection threshold and the calibration area, the sensitivity to these features should receive more attention in future studies.

An approximately linear relationship between contrail optical depths and radiative forcing was found. Assuming a globally constant $\tau = 0.3$ increases the radiative forcing by +140% (+270% including the longwave correction) in comparison with the reference experiment with a mean visible optical depth of 0.08. The true value of the global mean optical depth is difficult to obtain from observations. It may be approximated by combining observed and simulated probability distributions for regions where detailed observations are available. In view of the study of Kärcher et al. (2010), who determined the mean optical depth of all contrails over the USA by such an approach to be 0.125, it cannot be excluded that the radiative forcing as simulated with ECHAM may be significantly underestimated, assuming that the optical depth bias as determined for the USA is globally representative.

A strong influence on contrail radiative forcing was found when using an upgraded parameterisation of potential contrail coverage, yielding a strong increase of tropical contrails, in better agreement with observations. This enhances the global contrail radiative forcing by more than 50% with respect to the reference case.

The findings of the present study explain to a large degree the differences and uncertainties in recent contrail radiative forcing estimates. They demonstrate the importance of more reliable contrail observations most preferably for different regions, including detection efficiencies with respect to optical depths and their statistical distribution. Without this information the observations are of limited value for comparison with modelling studies. While modelling of contrails by means of a process-based contrail parameterisation (e.g., Burkhardt and Kärcher, 2009) without the need of calibration is most preferable, the need of well-documented observational data for the validation of such models still remains.

Modelling the full range of contrail optical depths including subvisible contrails is preferable over considering only visible ones, since the present study demonstrates that the radiative forcing of subvisible contrails should certainly not be neglected, as their contribution to the total contrail radiative forcing may exceed 30%.

All other factors which were investigated (model climate, air traffic inventory, air traffic density parameter, ice particle shape and diurnal variation of air traffic) are non-negligible, but within the present study only a moderate impact on global mean contrail

radiative forcing was found, resulting in relative changes of global mean net radiative forcing between −12% (model climate) and +14% (spherical particles) compared to the reference case. However, their impact on regional and seasonal contrail radiative forcing can be more distinct.

While the most important key factors for global contrail radiative forcing have been identified, providing a best estimate is beyond the scope of this study. Within our model framework an improved estimate of radiative forcing could be derived by employing the upgraded potential contrail coverage parameterisation, the model with superior climatology, an appropriate detection threshold for the calibration to observed contrail coverage, and including the diurnal cycle of air traffic. Such an estimate should be accompanied by an uncertainty range corresponding to those parameters which are not exactly known at present (e.g., the particle shape, air traffic inventory, and air traffic density parameter). In order to derive a best estimate in the sense of IPCC, results of different climate models and radiative transfer codes need to be combined, as the sensitivity of contrail radiative forcing between different models can be larger than the sensitivity to different parameters and setups within one model. Similarly an uncertainty range as inferred from one model would still represent only a part of the uncertainty range resulting from a variety of models.

Acknowledgements

The authors acknowledge funding from the EU FP6 NoE ECATS, the EU FP6 IP QUANTIFY, and the DLR project CATS. Thanks go to Christina Newinger (DLR) who kindly prepared the ERA40 humidity data, provided by ECMWF, and to Klaus Gierens (DLR) for helpful discussions. The simulations were run on the DKRZ NEC-SX6. This work is part of the first author's PhD thesis, published under her maiden name Christine Fichter.

References

Airbus, 2009. Airbus Global Market Forecast 2009–2028. Flying Smart, Thinking Big. Airbus, France. www.airbus.com.

Bakan, S., Betancor, M., Gayler, V., Graßl, H., 1994. Contrail frequency over Europe from NOAA-satellite images. Ann. Geophys. 12, 962–968.

Burkhardt, U., Kärcher, B., 2009. Process-based simulation of contrail cirrus in a global climate model. J. Geophys. Res. 114, D16201. doi:10.1029/2008JD011491.

Burkhardt, U., Kärcher, B., Ponater, M., Gierens, K., Gettelman, A., 2008. Contrail cirrus supporting areas in model and observations. Geophys. Res. Lett. 35, L16808. doi:10.1029/2008GL034056.

Eyers, C., Norman, P., Middel, J., Plohr, M., Michot, S., Atkinson, K., Christou, R., 2004. AERO2K Global Aviation Emissions Inventories for 2002 and 2025. Report number QinetiQ/04/01113, QinetiQ, Farnborough.

Fichter, C., Marquart, S., Sausen, R., Lee, D., 2005. The impact of cruise altitude on contrails and related radiative forcing. Meteorol. Z. 14 (4), 563–572. doi:10.1127/0941-2948/2005/0048.

Forster, P., Ramaswamy, V., Artaxo, P., Berntsen, T., Betts, R., Fahey, D., Haywood, J., Lean, J., Lowe, D., Myhre, G., Nganga, J., Prinn, R., Raga, G., Schulz, M., Van Dorland, R., 2007. Changes in Atmospheric Constituents and in Radiative Forcing. Climate Change 2007: The Physical Science Basis. Contribution of Working Group I to the Fourth Assessment Report of the Intergovernmental Panel on Climate Change. Cambridge University Press, Cambridge, UK. 129–234.

Gauss, M., Isaksen, I., Lee, D., Søvde, O., 2006. Impact of aircraft NO_x emissions on the atmosphere – tradeoffs to reduce the impact. Atmos. Chem. Phys. 6, 1529–1548.

Goodman, J., Pueschel, R., Jensen, E., Verma, S., Ferry, G., Howard, S., Kinne, S., Baumgardner, D., 1998. Shape and size of contrails ice particles. Geophys. Res. Lett. 25 (9), 1327–1330.

Kärcher, B., Burkhardt, U., Ponater, M., Frömming, C., 2010. Importance of representing optical depth variability for estimates of global line-shaped contrail radiative forcing. Proc. Natl. Acad. Sci. U.S.A. 107 (45), 19181–19184. doi:10.1073/pnas.1005555107.

Kärcher, B., Burkhardt, U., Unterstrasser, S., Minnis, P., 2009. Factors controlling contrail cirrus optical depth. Atmos. Chem. Phys. 9, 6229–6254.

Lee, D., Fahey, D., Forster, P., Newton, P., Wit, R., Lim, L., Owen, B., Sausen, R., 2009. Aviation and global climate change in the 21st century. Atmos. Environ. 43, 3520–3537. doi:10.1016/j.atmosenv.2009.04.024.

Leggett, J., Pepper, W., Swart, R., Edmonds, J., Meira Filho, L., Mintzer, I., Wang, M., Wasson, J., 1992. Emissions scenarios for the IPCC: an update. Climate Change 1992: The Supplementary Report to the IPCC Scientific Assessment, 69–95.

Mannstein, H., Meyer, R., Wendling, P., 1999. Operational detection of contrails from NOAA-AVHRR-data. Int. J. Remote Sens. 20 (8), 1641–1660.

Marquart, S., 2003. Klimawirkung von Kondensstreifen: Untersuchungen mit einem globalen atmosphärischen Zirkulationsmodell. Ph.D. thesis, Fakultät für Physik, Ludwig-Maximilians-Universität München, DLR Forschungsbericht 2003-16, ISSN 1434-8454, Köln, published in German.

Marquart, S., Mayer, B., 2002. Towards a reliable GCM estimation of contrail radiative forcing. Geophys. Res. Lett. 29 (8), 1179. doi:10.1029/2001GL014075.

Marquart, S., Ponater, M., Mager, F., Sausen, R., 2003. Future development of contrail cover, optical depth and radiative forcing: impacts of increasing air traffic and climate change. J. Climate 16 (17), 2890–2904.

Meerkötter, R., Schumann, U., Doelling, D., Minnis, P., Nakajima, T., Tsushima, Y., 1999. Radiative forcing by contrails. Ann. Geophys. 17 (8), 1080–1094.

Meyer, R., Buell, R., Leiter, C., Mannstein, H., Pechtl, S., Oki, T., Wendling, P., 2007. Contrail observations over Southern and Eastern Asia in NOAA/AVHRR data and comparisons to contrail simulations in a GCM. Int. J. Remote Sens. 28 (9), 2049–2069.

Minnis, P., Palikonda, R., Ayers, J., Duda, D., Costulis, K., 2000. Cirrus, contrails, and radiative forcing over the USA: their relationship to air traffic and upper troposphere conditions. A2C3 Conference Proceedings, Seeheim. European Commission, ISBN 92-894-0461-2, 193–196.

Minnis, P., Schumann, U., Doelling, D., Gierens, K., Fahey, D., 1999. Global distribution of contrail radiative forcing. Geophys. Res. Lett. 26 (13), 1853–1856.

Myhre, G., Kvalevag, M., Rädel, G., Cook, J., Shine, K., Clark, H., Karcher, F., Markowicz, K., Kardas, A., Wolkenberg, P., Balkanski, Y., Ponater, M., Forster, P., Rap, A., Rodriguez de Leon, R., 2009. Intercomparison of radiative forcing calculations of stratospheric water vapour and contrails. Meteorol. Z. 18 (6), 585–596. doi:10.1127/0941-2948/2009/0411.

Obermaier, K., 2007. Evaluierung der mit ECHAM4.L39(DLR)/ATTILA simulierten Wasserdampfverteilung im UT/LS-Bereich anhand von Beobachtungsdaten. Diploma thesis, Ludwigs-Maximilians-Universität München, 65p.

Palikonda, R., Minnis, P., Duda, D., Mannstein, H., 2005. Contrail coverage derived from 2001 AVHRR data over the continental United States of America and surrounding areas. Meteorol. Z. 14 (4), 525–536. doi:10.1127/0941-2948/2005/0051.

Penner, J., et al., 1999. Aviation and the Global Atmosphere: A Special Report of IPCC Working Groups I and III in Collaboration with the Scientific Assessment Panel to the Montreal Protocol on Substances that Deplete the Ozone Layer. Cambridge University Press, pp. 373.

Ponater, M., Marquart, S., Sausen, R., 2002. Contrails in a comprehensive global climate model: Parameterization and radiative forcing results. J. Geophys. Res. 107 (13), 4164. doi:10.1029/2001JD000429.

Rädel, G., Shine, K., 2008. Radiative forcing by persistent contrails and its dependence on cruise altitudes. J. Geophys. Res. 113, D07105. doi:10.1029/2007JD009117.

Rap, A., Forster, P., Jones, A., Boucher, O., Haywood, J., Bellouin, N., De Leon, R., 2010. Parameterisation of contrails in the UK Met Office Climate Model. J. Geophys. Res. 115, D10205. doi:10.1029/2009JD012443.

Reithmeier, C., Sausen, R., 2002. ATTILA: atmospheric tracer transport in a Lagrangian model. Tellus B 54 (3), 278–299.

Sausen, R., Gierens, K., Ponater, M., Schumann, U., 1998. A diagnostic study of the global distribution of contrails. Part I: Present day climate. Theor. Appl. Climatol. 61 (3), 127–141.

Schröder, F., Kärcher, B., Duroure, C., Ström, J., Petzold, A., Gayet, J., Strauss, B., Wendling, P., Borrmann, S., 2000. On the transition of contrails into cirrus clouds. J. Atmos. Sci. 57 (4), 464–480.

Schumann, U., 1996. On conditions for contrail formation from aircraft exhausts. Meteorol. Z. 5, 4–23.

Stenke, A., Grewe, V., Ponater, M., 2008. Lagrangian transport of water vapor and cloud water in the ECHAM4 GCM and its impact on the cold bias. Clim. Dyn. 31 (5), 491–506.

Stuber, N., Forster, P., 2007. The impact of diurnal variations of air traffic on contrail radiative forcing. Atmos. Chem. Phys. 7, 3153–3162.

Stuber, N., Forster, P., Rädel, G., Shine, K., 2006. The importance of the diurnal and annual cycle of air traffic for contrail radiative forcing. Nature 441 (7095), 864–867.

Stuber, N., Sausen, R., Ponater, M., 2001. Stratosphere adjusted radiative forcing calculations in a comprehensive climate model. Theor. Appl. Climatol. 68 (3), 125–135.